



Article

New Molecules of Diterpene Origin with Inhibitory Properties toward α -Glucosidase

Elena Tretyakova¹, Irina Smirnova¹, Oxana Kazakova^{1,*} , Ha Thi Thu Nguyen², Alina Shevchenko³, Elena Sokolova³ and Denis Babkov³

¹ Ufa Institute of Chemistry, Ufa Federal Research Centre, Russian Academy of Sciences, 71 Prospect Oktyabrya, 450054 Ufa, Russia

² Institute of Chemistry, Vietnamese Academy of Science and Technology, 18 Hoang Quoc Viet Str., Cau Giay Dist., Hanoi 100000, Vietnam

³ Scientific Center for Innovative Drugs, Volgograd State Medical University, Novorossiyskaya Str. 39, 400087 Volgograd, Russia

* Correspondence: obf@anrb.ru; Tel.: +7-347-235-6066

Abstract: The incidence of diabetes mellitus (DM), one of the most common chronic metabolic disorders, has increased dramatically over the past decade and has resulted in higher rates of morbidity and mortality worldwide. The enzyme, α -Glucosidase (α -GLy), is considered a therapeutic target for the treatment of type 2 DM. Herein, we synthesized arylidene, heterocyclic, cyanoethoxy- and propargylated derivatives of quinopimaric acid (levopimaric acid diene adduct with *p*-benzoquinone) **1–50** and, first, evaluated their ability to inhibit α -GLy. Among the tested compounds, quinopimaric acid **1**, 2,3-dihydroquinopimaric acid **8** and its amide and heterocyclic derivatives **9**, **30**, **33**, **39**, **44**, with IC₅₀ values of 35.57–65.98 μ M, emerged as being good inhibitors of α -GLy. Arylidene 1 β -hydroxy and 1 β ,13 α -epoxy methyl dihydroquinopimarate derivatives **6**, **7**, **26–29**, thiadiazole **32**, 1a,4a-dehydroquinopimaric acid **40** and its indole, nitrile and propargyl hybrids **35–38**, **42**, **45**, **48**, and **50** showed excellent inhibitory activities. The most active compounds **38**, **45**, **48**, and **50** displayed IC₅₀ values of 0.15 to 0.68 μ M, being 1206 to 266 more active than acarbose (IC₅₀ of 181.02 μ M). Kinetic analysis revealed the most active diterpene indole with an alkyne substituent **45** as a competitive inhibitor with K_i of 50.45 μ M. Molecular modeling supported this finding and suggested that the indole core plays a key role in the binding. Compound **45** also has favorable pharmacokinetic and safety properties, according to the computational ADMET profiling. The results suggested that quinopimaric acid derivatives should be considered as potential candidates for novel alternative therapies in the treatment of type 2 diabetes.

Keywords: diabetes mellitus; α -glucosidase; abietane diterpenoids; levopimaric acid; quinopimaric acid; molecular docking; ADMET



Citation: Tretyakova, E.; Smirnova, I.; Kazakova, O.; Nguyen, H.T.T.; Shevchenko, A.; Sokolova, E.; Babkov, D.; Spasov, A. New Molecules of Diterpene Origin with Inhibitory Properties toward α -Glucosidase. *Int. J. Mol. Sci.* **2022**, *23*, 13535. <https://doi.org/10.3390/ijms232113535>

Academic Editors: Simona Gabriela Bungau and Vesa Cosmin

Received: 12 October 2022

Accepted: 1 November 2022

Published: 4 November 2022

Publisher's Note: MDPI stays neutral with regard to jurisdictional claims in published maps and institutional affiliations.



Copyright: © 2022 by the authors. Licensee MDPI, Basel, Switzerland. This article is an open access article distributed under the terms and conditions of the Creative Commons Attribution (CC BY) license (<https://creativecommons.org/licenses/by/4.0/>).

1. Introduction

Enzymes responsible for breaking down proteins, carbohydrates and lipids into smaller and more readily absorbable molecules are a key component of the digestive system. The main cause of many metabolic diseases is abnormal changes in the activity of these enzymes. Inhibition of metabolic enzymes, such as α -glucosidase (α -GLy), is one of the accepted approaches in the treatment of diabetes mellitus (DM), which is one of the most common chronic endocrine diseases, along with arterial hypertension and obesity [1]. The number of people with disorders of carbohydrate metabolism and the incidence of DM are constantly growing, which is primarily due to an increase in the number of patients with obesity, as well as in average life expectancy [2]. Type II diabetes mellitus (DM2), accounting for about 90% of all cases of diabetes, is caused by a decrease in insulin sensitivity in target organs, such as the liver, muscle, and adipose tissue, as well as a deficiency in insulin secretion [3–5]. Medicinal agents with the ability to stimulate glucose uptake in these

tissues can be used to improve insulin resistance and, therefore, to treat DM2 [6]. Today, a vast number of synthetic antidiabetic agents, such as acarbose, miglitol, sulfonylurea, metformin, and thiozolidinedione, are readily available on the market [7–9]. However, their effectiveness is limited, due to low bioavailability and unwanted side effects [10–12]. Therefore, there is a great need to develop alternative and more active antidiabetic drugs from natural sources.

Abietane diterpenoids are classes of compounds which are mainly found in the conifer family and have long been used to treat a variety of ailments [13]. Their derivatives are characterized by a wide range of biological activities, like anticancer, antiviral, antimicrobial, antileishmanial, antiplasmodial, antifungal, antitumour, cytotoxicity, antiulcer, cardiovascular, antioxidant, anti-inflammatory and antidiabetic activities [14–21]. Abietic and dehydroabietic acids have been reported to decrease the activity of glucose-6-phosphatase and to stimulate glycogen synthase [22]. Carnosic acid derivatives are very effective in treating diabetic complications by improving insulin secretion [23] and glucose homeostasis or by stimulating glucose uptake by increasing peripheral glucose clearance in tissues [24]. Abietic and carnosic acids also significantly activate nuclear receptor peroxisome proliferator-activated receptor PPAR- γ by exerting its beneficial effect on lipid and glucose homeostasis through PPAR- γ -mediated pathways [25,26]. Carnosol stimulates glucose uptake [27], improves diabetes and its complications by the regulation of oxidative stress and inflammatory responses [28] and suppresses forskolin-induced luciferase expression, when monitored by the cAMP/response element, and glucose-6-phosphatase gene promoters [29–31]. Tanshinones exhibited potent protein tyrosine phosphatase 1B inhibitory activity [32] as well as increased the activity of insulin on the tyrosine phosphorylation of the insulin receptor in addition to the activation of the kinases Akt, ERK1/2, and GSK3beta and may be very useful for developing new anti-diabetic agents as specific insulin receptor activators [33].

Studies evaluating the antidiabetic properties of abietane diterpenoids in an animal model using rats and mice showed that dehydroabietic acid reduces plasma glucose and insulin levels, as well as plasma and hepatic triglyceride levels, by suppressing the production of monocyte chemoattractant protein-1 and tumor necrosis factor-alpha and increasing that of adiponectin, through decrease in macrophage infiltration into adipose tissues [34]. Carnosol and carnosic acid reduced plasma glucose, total cholesterol, and triglycerides in a diabetic group of rats and suppressed inflammation and lipogenesis in mice administered a high-fat diet, through C-kinase substrate regulation [23,28,35]. Tanshinone analogs also demonstrated a significant decrease in blood glucose level, total cholesterol and triglyceride, free fatty acids, and insulin receptor substrate 1 expression, body weight loss and higher insulin resistance when administered to type 2 diabetic rats, with oral administration, resulting in the activation of AMP-activated protein kinase in aortas from ob/ob or db/db mice [35,36]. Data on systematic studies of the enzymatic activity of abietane diterpenoid derivatives, obtained as a result of various modifications of the native core, in particular, on levopimaric acid derivatives as potential inhibitors of α -GLy, are practically absent in the literature. Therefore, herein, we describe the synthesis of abietane type derivatives with arylidene, heterocyclic, nitrile and acetylene fragments. These derivatives were, then, first evaluated for in-vitro α -GLy inhibition. The mechanism of inhibition and enzyme binding were investigated with kinetic and molecular modeling approaches.

2. Results and Discussion

2.1. Chemistry

Since the quinopimaric acid structure (the Diels-Alder reaction product of levopimaric acid and *p*-benzoquinone) contains major reaction centers at the C-1, C-3, C-4, and C-20 atoms, we planned to functionalize these positions for better understanding of the structure–activity relationship and to reveal new promising molecules with antidiabetic activity (Figure 1).

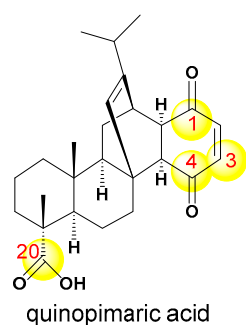


Figure 1. Quinopimaric acid reaction centers for the SAR studies of the current research.

Modifications of these sites involved the synthesis of arylidene and heterocyclic derivatives and quinopimaric acid cyanoethoxy- and propargylated analogs. Figure 2 shows the structures of quinopimaric acid **1** and its analogs **2–30**, modified at position C-1, C-3, C-4, and C-20.

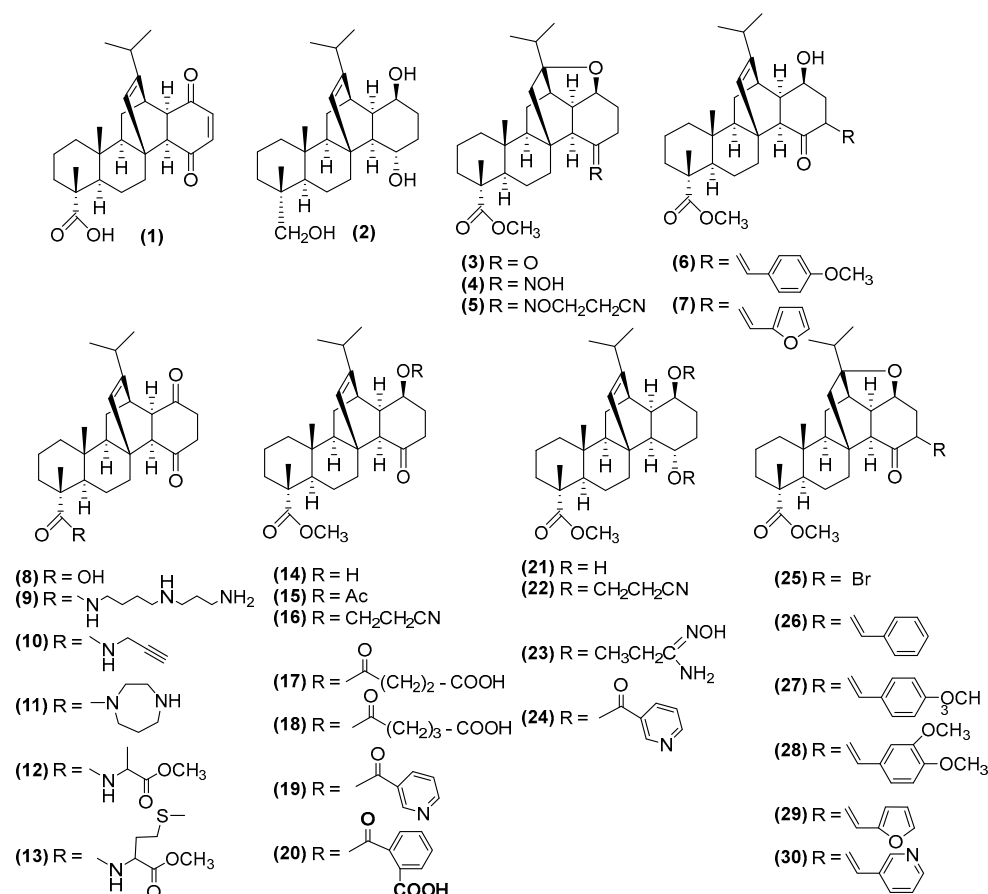


Figure 2. Structures of quinopimaric acid **1** and its analogs **2–30**, modified at position C-1, C-3, C-4, and C-20.

Figure 3 shows the structures of quinopimaric acid heterocyclic derivatives obtained as a result of interaction with hydrazine hydrate **31**, thiourea **32**, and using the Fischer reaction (indoles **33**, **34**), Nenitzescu reaction (indoles **35–38**) and Beckmann rearrangement (lactam **39**).

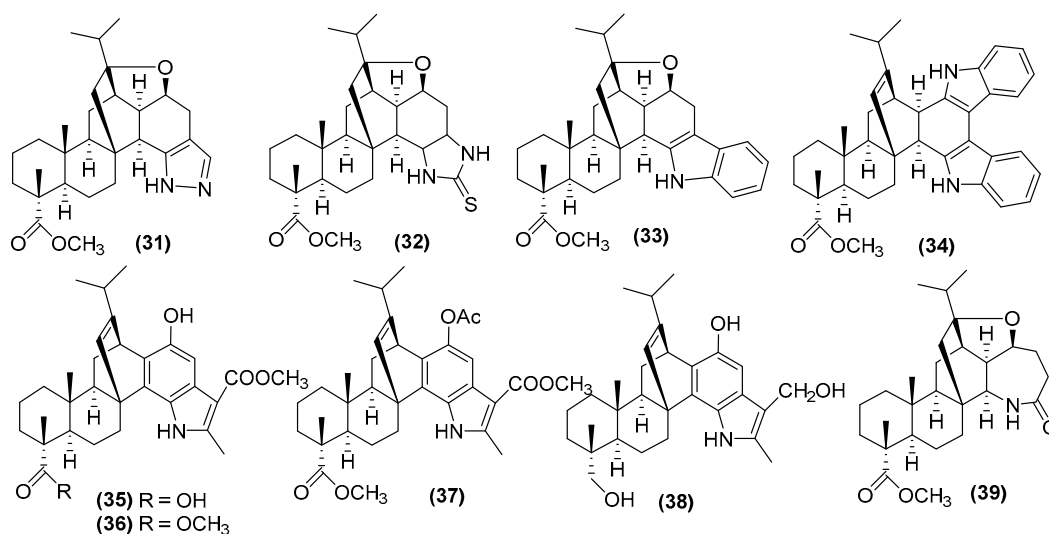
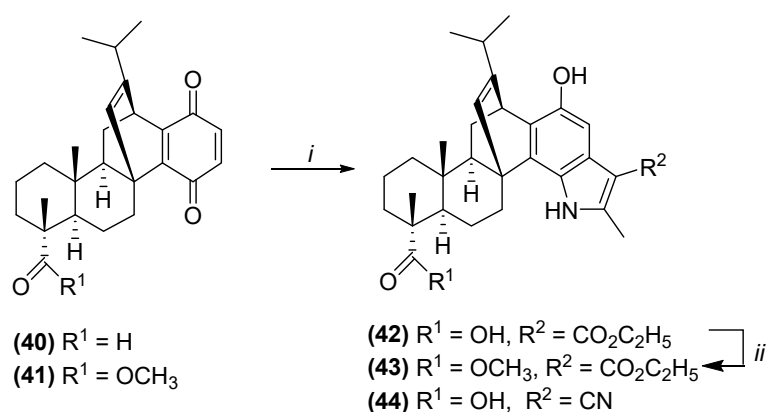


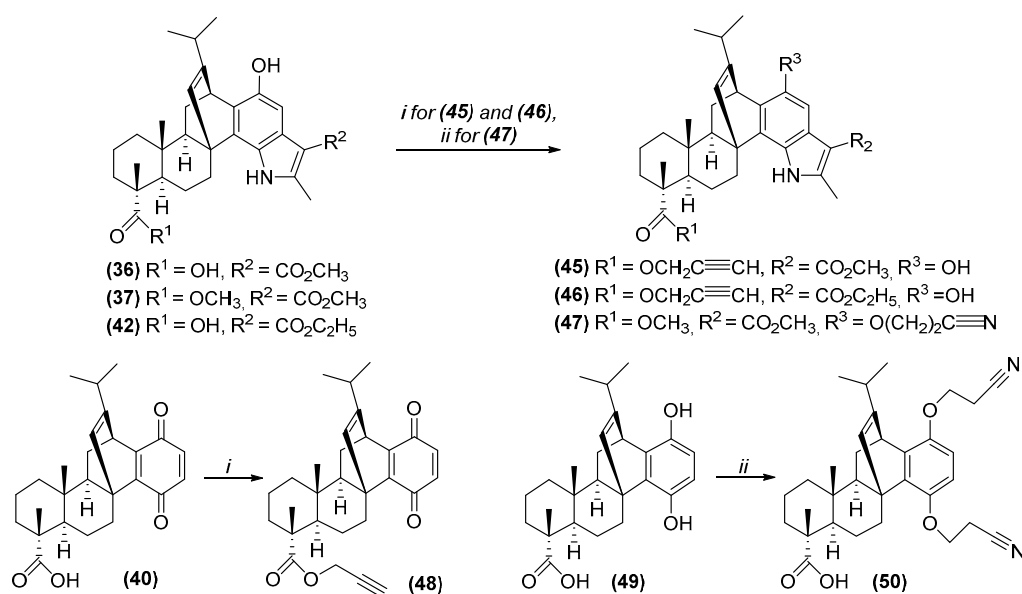
Figure 3. Structures of quinopimaric acid heterocyclic derivatives 31–39.

We planned to use the Nenitzescu reaction [37] for the synthesis of new diterpene indoles. In this reaction, 1a,4a-dehydroquinopimaric acid **40**, easily formed in two steps from quinopimaric acid **1** [38], was used as the quinone component, as well as ethyl 3-aminocrotonate or 3-aminocrotononitrile being used as the new enamine components. Under the conditions of the Nenitzescu indole synthesis by the reaction of 1a,4a-dehydroquinopimaric acid **40** with the corresponding enamine in glacial AcOH, at room temperature, diterpene indoles **42**, **44** were synthesized in 76 and 69% yields, respectively. Methyl ester of diterpene indole **43** was obtained in quantitative yield by treating compound **42** with methyl iodide during reflux in acetone for 2 h in the presence of potash (Scheme 1), or direct synthesis from 1a,4a-dehydroquinopimaric acid methyl ester **41**, similar to the preparation of compounds **42** and **44**.



Scheme 1. Synthesis of new diterpene indoles **42–44** by Nenitzescu reaction. Reagents and conditions: (i) ethyl 3-aminocrotonate for **42**, **43** or 3-aminocrotononitrile for **44**, AcOH, rt, 20 h; (ii) CH_3I , K_2CO_3 , acetone, reflux, 2 h.

Propargyl derivatives **45**, **46**, **48** were obtained in 79–83% yields by the reaction of diterpene indoles **36**, **43** and quinone **40** with propargyl bromide during reflux in dimethylformamide in the presence of K_2CO_3 . Cyanoethoxy derivatives **47**, **50** were prepared by adding acrylonitrile in 1,4-dioxane, at room temperature, to the diterpene indole **37** or aromatic derivative **49** in the occurrence of phase transfer catalyst triethylbenzylammonium chloride in combination with an alkali (30% KOH) (Scheme 2).



Scheme 2. Synthesis of propargyl **45**, **46**, **48** and cyanoethoxy **47**, **50** quinopimaric acid derivatives. Reagents and conditions: (i) propargyl bromide, DMF, K_2CO_3 , reflux, 2 h; (ii) acrylonitrile, 1,4-dioxane, KOH, BTAC, rt, 2 h.

The structures of the synthesized compounds were confirmed using mass spectrometry, and one- and two-dimensional (COSY, NOESY, ^1H - ^{13}C HSQC, ^1H - ^{13}C HMBC) NMR spectroscopy. Thus, the signal of the C-2 carbon atom of the aromatic ring in the ^{13}C NMR spectra of compound **42**–**44** appeared at δ 99.7–103.3 ppm, and correlated with the signal of the H-2 proton at δ 6.83–7.28 ppm in the ^1H - ^{13}C HSQC spectra. The ^1H NMR spectra showed characteristic signals of methyl group protons at δ 2.51–2.71 (3'-CH₃), as well as broadened signals of the hydroxyl group and NH group at δ 9.12–9.35 and 12.13 ppm, respectively. The ^1H NMR spectra of compound **43** contained an additional signal of the protons of the methyl ester group at δ 3.76 ppm, which, in the ^1H - ^{13}C HSQC spectrum, correlated with the signal of the C-21 atom at δ 15.5 ppm. In the ^{13}C NMR spectra of compound **44**, a carbon signal of the CN-group was observed at δ 117.8 ppm. The ^1H NMR spectra of propargyl derivatives **45**, **46**, **48** contained the methylene group proton signal in the region δ 4.67–4.82 ppm, while in the ^{13}C NMR the triple bond carbon signals appeared at δ 74.4–74.9 and 77.9–79.3 ppm, respectively. The signals of the cyanoethyl methylene groups in the ^1H NMR spectra of compounds **47**, **50** were observed in the region δ 2.80–2.91 and 4.05–4.30 ppm, and the characteristic carbon signal of the nitrile group in the ^{13}C NMR spectra was observed at δ 117.4–117.6 ppm (Figures S1–S18, Supplementary Materials).

2.2. Inhibition of Yeast α -Glucosidase

All the synthesized compounds **1**–**50** were tested for their inhibitory potential against yeast α -GLy. Acarbose served as a control drug in this experiment. The IC_{50} values of compounds are provided in Table 1.

Quinopimaric acid derivatives **2**–**5**, **10**–**25**, **27**, **31**, **34**, **41**, **43**, **46**, **49** showed moderate to poor α -GLy inhibition. Quinopimaric acid **1**, 2,3-dihydroquinopimaric acid **8** and its amide and heterocyclic derivatives **9**, **30**, **33**, **39**, **44**, with an IC_{50} value of 35.24 ± 0.71 Mm— 65.98 ± 0.03 μM , emerged as good inhibitors of α -GLy. Arylidene 1 β -hydroxy and 1 β ,13-epoxy methyl dihydroquinopimarate derivatives **6**, **7**, **26**–**29**, thiadiazole **32**, 1a,4a-dehydroquinopimaric acid **40** and its indole, nitrile and propargyl hybrids **35**–**38**, **42**, **45**, **48**, and **50** showed excellent inhibitory activities. The most active compounds, **38**, **45**, **48**, and **50**, displayed IC_{50} values of 0.15 ± 0.008 μM to 0.68 ± 0.045 μM , being 1206 to 266 more potent than acarbose (IC_{50} of 181.02 ± 3.1 μM).

Table 1. α -Glucosidase inhibitory potential of the synthesized compounds 1–50.

Compound	IC ₅₀ ± SE (μM)
1	59.59 ± 0.18
2	>255
3	>255
4	>255
5	>255
6	1.63 ± 0.006
7	2.50 ± 0.011
8	35.57 ± 0.92
9	35.24 ± 0.71
10	>255
11	>255
12	>255
13	>255
14	>255
15	>255
16	>255
17	>255
18	>255
19	>255
20	>255
21	>255
22	>255
23	>255
24	>255
25	>255
26	13.08 ± 0.01
27	>255
28	12.73 ± 0.21
29	1.63 ± 0.041
30	38.80 ± 0.33
31	>255
32	9.66 ± 0.77
33	65.98 ± 0.03
34	>255
35	7.95 ± 0.20
36	8.94 ± 0.96
37	7.28 ± 0.40
38	0.39 ± 0.03
39	44.77 ± 0.96
40	7.088 ± 0.12
41	>255
42	2.52 ± 0.34
43	>255
44	68.22 ± 0.03
45	0.15 ± 0.008
46	>255
47	4.95 ± 0.25
48	0.68 ± 0.045
49	>255
50	0.23 ± 0.01
Acarbose (reference drug)	181.02 ± 3.1

As shown in Table 1, quinopimaric acid **1** had an activity against α -Gly three times higher than that of acarbose. Its simplest modifications, namely, the reduction of the C2-C3 bond (compound **8**), led to an increase in activity, and the introduction of a double bond into the C1a-C4a position (compound **40**) further enhanced this. Modifications at positions C-1, C-4, C-20 of dihydroquinopimaric acid (compounds **2–5**, **9–14**, **15–24**) were unsuccessful and led to a complete loss of activity. However, the introduction of arylidene substituents

into the C-3 position of 1 β ,13 α -epoxy methylhydroquinopimarate **3** (compounds **26**, **28–30**) resulted mainly in active compounds, and the most successful, for this series of compounds, was the presence of a furfural fragment in the molecule. Heterocyclization of dihydroquinopimaric acid (compounds **31–34**, **39**) led to compounds with high activity against α -GLy only in the case of thiadiazole **32** and indole **34**.

The use of acid **40** as a starting compound for heterocyclization provided more active compounds. Indole and its derivatives **35–38** showed excellent activity, especially alcohol **38**. Inspired by these results, we carried out the synthesis of new indoles using other enamines. The obtained two new indoles **42** and **44** also had very good activity, and it was better for the indole with an ethyl substituent. Modification of the C-20 position by introducing a triple bond into the molecule (compounds **45**, **46**), and the C-1 position with a cyanoethyl fragment (compound **47**) in the case of indole **36**, further enhanced this activity.

Thus, from the studied series of 50 compounds synthesis of indoles based on 1a,4a-dehydroquinopimaric acid **40** proved to be the most successful approach to obtain highly active α -GLy inhibitors. Modification, according to the Nenitzescu reaction, and reduction of carboxyl and methoxycarboxyl groups, with the formation of trihydroxy derivative **38**, propargylation of C-20 positions in acid **40** and indole **36**, as well as cyanoethylation of the aromatic derivative **49**, realized compounds with IC₅₀ values < 1 μ M.

For compounds **38**, **45**, **48** and **50**, which showed the highest activity against α -GLy, studies of their anti-oxidant, antimicrobial and cytotoxic activity were carried out (Tables S1–S3, see Supplementary Materials).

2.3. The Mechanism of α -Glucosidase Inhibition by Compound **45**

The mechanism of action for the most active diterpene indole with an alkyne substituent **45** was determined in a kinetic experiment using different 4-nitrophenyl β -D-glucopyranoside (pNPG) substrate concentrations. Nonlinear regression of kinetic curves, using the Michaelis–Menten equation (Figure 4), revealed that higher inhibitor concentrations increased K_m , while V_{max} remained constant, which rendered compound **45** as a competitive inhibitor. The inhibition constant K_i was estimated as 50.45 μ M.

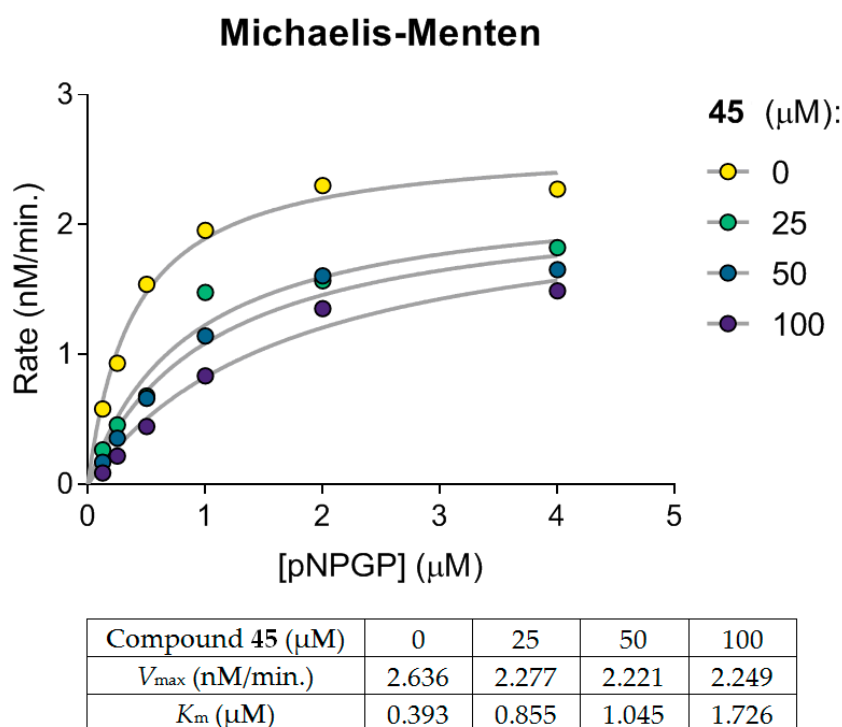


Figure 4. Michaelis–Menten kinetics for compound **45** indicates a competitive inhibition. The experiment was performed in two independent series.

The literature data regarding the mechanism of α -glucosidase inhibition for diterpenes is scarce. The majority of reported compounds are non-competitive inhibitors, e.g., entatisane-3-oxo-16 β ,17-acetonide [39], (E)-labda-8(17),12-diene-15,16-dial [40], ent-kaurane derivative of chepraecoxin A [41], and bis-labdanic diterpene were reported as mixed-type inhibitors [42]. Notably, these inhibitors share an alicyclic core. In contrast, diterpene carnosol, comprising aromatic catechol moiety, is a competitive inhibitor [43]. Aromatic rings of carnosol and compound **45** favor π -stacking interaction with phenylalanine, tyrosine, or tryptophan side chains [44], which might result in distinct binding patterns and inhibition kinetics.

2.4. Docking Studies for Compound **45**

We performed a molecular modeling study to gain insight into the structural basis of interactions between the lead compound **45** and α -Gly enzyme. Since “structure cannot be predicted from kinetics” [45], we avoided preconceived competitive mechanism assumptions and subjected the whole protein surface to a docking procedure (Figure 5).

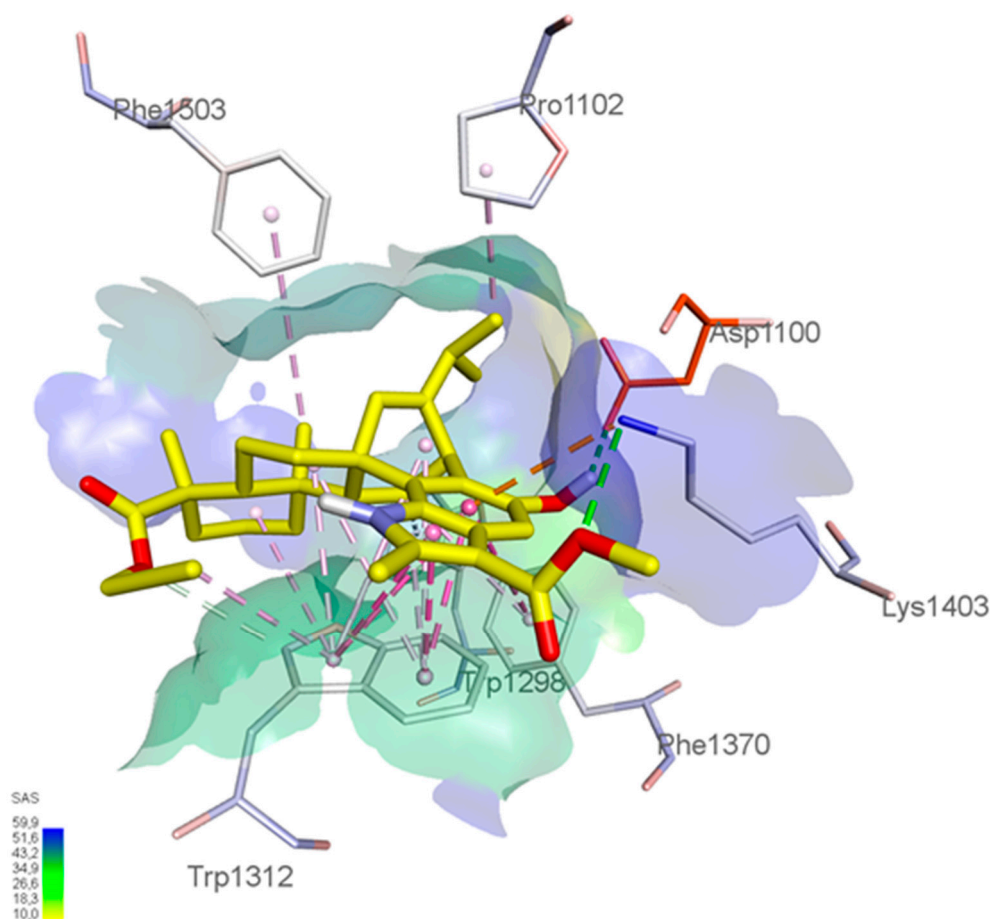


Figure 5. Proposed binding mode of compound **45** to yeast α -glucosidase. The inhibitor is shown in yellow carbons, catalytic Asp1100 is shown in orange carbons. Surface visualized solvent-accessible area. Dashed lines indicate key interactions with enzyme amino acids.

Nevertheless, docking proposed that diterpene derivative **45** shared a favorable binding site with acarbose. Moreover, the indole hydroxyl group appeared to form a conventional H-bond with carboxyl of the catalytic Asp1100 residue. The indole core itself contributed to the binding the most. It was anchored by strong π - π parallel stacking with a Trp1312 side chain and T-shaped π -stacking with a Phe1370 side chain. The amino group of Lys1403 formed an H-bond with the ester substituent and charged π -cation interaction with the indole aromatic system. The dodecahydrophenanthrene part of the molecule was also stabilized by Van

der Waals forces with multiple lipophilic residues (Pro1102, Trp1298, Trp1312, Phe1503). Both ester moieties of compound **45** pointed towards the solvent-accessible area of the pocket, providing an opportunity for the introduction of polar fragments. This modification might improve water solubility without hampering enzyme binding. To sum up, molecular modeling confirmed the competitive mechanism of action revealed in the kinetic experiment and provided guidance for future structural optimization.

2.5. ADMET Profiling of Compound **45**

We assessed drug-like, pharmacokinetic and toxicological properties of the lead compound **45** using a consensus of predictive services that took into account different computational strategies (Table 2).

Table 2. ADMET properties predicted for compound **45**.

Property	ADMETlab [46]	ADMETlab 2.0 [47]	SwissADME [48]	ProTox-II [49]	Consensus Value
Physicochemical					
Water solubility (µg/mL)	1.94	2.57	0.02		1.51
LogP	6.21	4.93	6.30	6.69	5.81
Absorption					
Human intestinal absorption	Yes	No	Low		No
Human oral bioavailability	No	No			No
Caco-2 permeability	Yes	No			–
P-glycoprotein substrate	No	No	No		No
P-glycoprotein inhibitor	Yes	Yes			Yes
Distribution					
Plasma protein binding (%)	87.09	99.83			93.46
BBB permeability	No	No	No		No
Metabolism					
CYP1A2 inhibitor	No	No	No		No
CYP2C19 inhibitor	Yes	Yes	No		Yes
CYP2C9 inhibitor	Yes	Yes	Yes		Yes
CYP2D6 inhibitor	No	Yes	No		No
CYP2D6 substrate	No	No			No
CYP3A4 inhibitor	Yes	Yes	No		Yes
CYP3A4 substrate	Yes	Yes			Yes
Excretion					
Total Clearance (mL/min/kg)	1.77	4.03			2.9
T _{1/2} (h)	2.13	0.15			1.14
Toxicity					
AMES toxicity	No	No		No	No
hERG inhibitor	Yes	No			–
Rat acute oral LD ₅₀ (mg/kg)	121.4			520	320.7
Hepatotoxicity	Yes	No		No	No
Skin Sensitisation	No	No			No
Carcinogenicity		No		No	No

Compound **45** fulfilled Lipinski's rule of 5 (with the exception of molecular weight <500) and Pfizer's rules. At the same time, GSK and "Golden triangle" rules were violated. Mean water solubility was acceptable. Importantly, there was a good consensus on low intestinal absorption and oral bioavailability, which could avoid systemic exposure to the substance. In the case of entering systemic circulation, indole **45** was anticipated to be bound to plasma proteins, likely due to high lipophilicity. Blood–brain barrier penetration was unlikely. Liver metabolism was to be mediated by cytochrome P450 3A4. Acute oral toxicity was predicted to be sufficiently low to achieve a wide therapeutic window. There were no alerts for toxicity to the liver and heart, nor mutagenicity and carcinogenicity. Hence, compound **45**'s calculated ADMET profile was favorable for the proposed mechanism of action.

3. Materials and Methods

3.1. General

The spectra were recorded at the Center for the Collective Use "Chemistry" of the UIC UFRC RAS and RCCU "Agidel" of the UFRC RAS. ¹H and ¹³C-NMR spectra were recorded

on a “Bruker AM-500” (Bruker, Billerica, MA, USA, 500 and 125.5 MHz respectively, δ , ppm, Hz) in CDCl_3 , internal standard tetramethylsilane. Melting points were detected on a micro table “Rapido PHMK05” (Nagema, Dresden, Germany). Optical rotations were measured on a polarimeter “Perkin-Elmer 241 MC” (Perkin Elmer, Waltham, MA, USA) in a tube length of 1 dm. Elemental analysis was performed on a Euro EA-3000 CHNS analyzer (Eurovector, Milan, Italy); the main standard was acetanilide. Thin-layer chromatography analyses were performed on Sorbfil plates (Sorbpolimer, Krasnodar, Russian Federation), using the solvent system chloroform–ethyl acetate, 40:1. Substances were detected by 10% H_2SO_4 with subsequent heating to 100–120 °C for 2–3 min. All the reagents and solvents were purchased from standard commercial vendors and were used without any further purification. For the synthesis of quinopimaric acid **1** [38] pine resin *Pinus silvestris* (containing about 25% levopimaric acid) was used. Compounds **2**, **14**, **15**, **17–21**, **24** [50], **3** [51], **4** [52], **5** [53], **6**, **9**, **11**, **26–28**, **30** [16], **7** [54], **8** [50], **10** [55], **12**, **13** [56], **16** [15], **22**, **23** [57], **25** [58], **29** [59], **31**, **32**, **34** [60], **33** [14], **35** [61], **36–39** [38], **40**, **49** [62] were obtained according to the methods previously described.

3.2. Synthesis of Compounds **42** and **44**

A threefold excess of ethyl 3-aminocrotonate (0.387 g, 3 mmol) or 3-aminocrotononitrile (0.246 g, 3 mmol) was added with stirring to a solution of compound **40** (0.408 g, 1 mmol) in glacial AcOH (20 mL). The reaction mixture was stirred at room temperature for 20 h, and then poured into H_2O . The precipitate was filtered off, washed until neutral, and the residue was air-dried. The reaction product was chromatographed on a silica gel column, eluent CHCl_3 –MeOH, 40: 1.

1-Hydroxy-13-isopropyl-1'-(ethoxycarbonyl)-7,10a,2'-trimethyl-5,6,6b,7,8,9,10,10a, 10b, 11,12,13-dodecahydro-12,4b-ethenophenanthro-[2,1-g]indole-7-carboxylic acid (**42**). Yield 0.395 g (76%), mp 131–133 °C, $[\alpha]_{\text{D}19} + 12.2^\circ$ (c 1.5, CHCl_3). ^1H NMR spectrum, δ , ppm (J, Hz): 0.79 (3H, s, 18- CH_3); 0.86–0.99 (1H, m, 10- CH_2); 1.18 (3H, d, J = 7.0, 17- CH_3); 1.22 (3H, d, J = 7.0, 16- CH_3); 1.29 (3H, s, 19- CH_3); 1.22–1.69 (10H, m, 6,8,9,10,11- CH_2 , 10b-CH); 1.77–1.80 (1H, m, 6b-CH); 1.98–2.18 (1H, m, 15-CH); 2.45–2.58 (1H, m, 5- CH_2); 2.67 (3H, s, 3'- CH_3); 2.82–2.91 (1H, m, 5- CH_2); 3.45 (3H, s, 6'- CH_3); 4.27 (1H, s, 12-CH); 4.31–4.35 (2H, m, 5'- CH_2); 5.68 (1H, s, 14-CH); 7.13 (1H, s, 2-CH); 9.65 (2H, br. s, OH); 9.80 (1H, br. s, NH). ^{13}C NMR spectrum, δ , ppm: 14.9 (C-3'); 16.4 (C-19); 16.7 (C-9), 17.2 (C-18); 20.5 (C-17); 20.8 (C-16); 22.0 (C-6); 28.3 (C-11); 32.0 (C-15); 33.5 (C-5); 36.1 (C-12); 36.8 (C-8); 38.2 (C-4b); 38.9 (C-10); 46.5 (C-7); 46.6 (C-10a); 49.8 (C-6b); 50.3 (C-6'); 54.9 (C-10b); 60.2 (C-5'), 102.9 (C-2); 108.0 (C-1'); 124.5 (C-3); 127.5 (C-13); 131.1 (C-1a); 133.6 (C-4a); 143.3 (C-4); 146.8 (C-1); 153.2 (C-14); 162.8 (C-2'); 165.3 (C-4'); 183.1 (C-20). Mass spectrum, m/z (Irel, %): 520 $[\text{M}+\text{H}]^+$ (100). Found, %: C 73.95; H 7.92; N 2.68. $\text{C}_{32}\text{H}_{41}\text{NO}_5$. Calculated, %: C 73.96; H 7.95; N 2.70.

1'-Cyano-1-hydroxy-13-isopropyl-7,10a,2'-trimethyl-5,6,6b,7,8,9,10,10a,10b,11,12,13-dodecahydro-12,4b-ethenophenanthro [2,1-g]indole-7-carboxylic acid (**44**). Yield 0.32 g (69%), mp 127–129 °C, $[\alpha]_{\text{D}19} + 25.5^\circ$ (c 1.0, CHCl_3). ^1H NMR spectrum, δ , ppm (J, Hz): 0.78 (3H, s, 18- CH_3); 0.82–0.95 (1H, m, 10- CH_2); 1.18 (3H, d, J = 7.0, 17- CH_3); 1.20 (3H, d, J = 7.0, 16- CH_3); 1.25 (3H, s, 19- CH_3); 1.22–1.69 (10H, m, 6,8,9,10,11- CH_2 , 10b-CH); 1.77–1.80 (1H, m, 6b-CH); 1.98–2.18 (1H, m, 15-CH); 2.45–2.58 (1H, m, 5- CH_2); 2.51 (3H, s, 3'- CH_3); 2.55–2.85 (1H, m, 5- CH_2); 4.31 (1H, s, 12-CH); 5.65 (1H, s, 14-CH); 6.55–6.83 (1H, m, 2-CH); 9.35 (3H, br. s, OH, NH). ^{13}C NMR spectrum, δ , ppm: 12.8 (C-3'); 16.4 (C-19); 16.7 (C-9), 17.1 (C-18); 20.1 (C-17); 20.3 (C-16); 22.0 (C-6); 28.1 (C-11); 32.0 (C-15); 34.6 (C-5); 36.8 (C-12); 37.6 (C-8); 38.2 (C-4b); 38.8 (C-10); 46.3 (C-7); 46.8 (C-10a); 49.9 (C-6b); 55.2 (C-10b); 83.3 (C-1'); 99.7 (C-2); 117.8 (C-4'); 124.4 (C-3); 126.8 (C-1a); 127.1 (C-14); 130.9 (C-4); 134.4 (C-4a); 144.3 (C-1); 146.4 (C-13); 153.7 (C-2'); 182.5 (C-20). Mass spectrum, m/z (Irel, %): 473 $[\text{M}+\text{H}]^+$ (100). Found, %: C 76.22; H 7.65; N 5.90. $\text{C}_{30}\text{H}_{36}\text{N}_2\text{O}_3$. Calculated, %: C 76.24; H 7.68; N 5.93.

3.3. Synthesis of Methyl 1-Hydroxy-13-Isopropyl-1'-(Ethoxycarbonyl)-7,10a,2'-Trimethyl-5,6,6b,7,8,9,10,10a,10b,11,12,13-Dodecahydro-12,4b-Ethenophenanthro-[2,1-g]indole-7-Carboxylate (**43**)

Procedure A. Methyl iodide (2 mL) and potassium carbonate (0.21 g) were added to a solution of **40** (0.408 g, 1 mmol) in acetone (15 mL), and the mixture was heated to reflux for 2 h. The reaction mixture was filtered. The filtrate was evaporated under reduced pressure, and the residue was purified on a silica gel column, eluent hexane–ethyl acetate, 5:1.

Procedure B. A threefold excess of 3-aminocrotononitrile (0.246 g, 3 mmol) was added with stirring to a solution of compound **41** (0.422 g, 1 mmol) in glacial AcOH (20 mL). The reaction mixture was stirred at room temperature for 20 h, and then poured into H₂O. The precipitate was filtered off, washed until neutral, and the residue was air-dried. The reaction product was chromatographed on a silica gel column, eluent CHCl₃–MeOH, 40: 1.

Yield 0.45 g (85%), mp 120–122°C, [α]_{D19} +12.9° (c 0.75, CHCl₃). ¹H NMR spectrum, δ , ppm (J, Hz): 0.79 (3H, s, 18-CH₃); 0.86–0.99 (1H, m, 10-CH₂); 1.18 (3H, d, J = 7.0, 17-CH₃); 1.22 (3H, d, J = 7.0, 16-CH₃); 1.29 (3H, s, 19-CH₃); 1.22–1.69 (10H, m, 6,8,9,10,11-CH₂, 10b-CH); 1.40–1.43 (3H, s, 6'-CH₃); 1.77–1.80 (1H, m, 6b-CH); 1.98–2.18 (1H, m, 15-CH); 2.45–2.58 (1H, m, 5-CH₂); 2.73 (3H, s, 3'-CH₃); 2.85–3.15 (1H, m, 5-CH₂); 3.76 (3H, s, 21-CH₃), 4.27 (1H, s, 12-CH); 4.31–4.39 (2H, m, 5'-CH₂); 5.71 (1H, s, 14-CH); 7.28 (1H, s, 2-CH); 5.95 (1H, br. s, NH); 12.13 (1H, br. s, OH). ¹³C NMR spectrum, δ , ppm: 14.9 (C-3'); 15.5 (C-21), 16.4 (C-19); 16.8 (C-9), 17.2 (C-18); 20.2 (C-17); 20.5 (C-16); 22.1 (C-6); 28.3 (C-11); 32.2 (C-15); 33.2 (C-5); 36.3 (C-12); 36.9 (C-8); 38.4 (C-4b); 38.9 (C-10); 46.6 (C-7); 47.4 (C-10a); 49.9 (C-6b); 52.0 (C-6'); 54.8 (C-10b); 60.3 (C-5'), 103.3 (C-2); 108.2 (C-1'); 124.7 (C-3); 127.6 (C-13); 130.9 (C-1a); 133.6 (C-4a); 143.6 (C-4); 146.4 (C-1); 153.1 (C-14); 162.9 (C-2'); 165.2 (C-4'); 179.7 (C-20). Mass spectrum, m/z (I_{rel}, %): 534 [M] + (100). Found, %: C 74.25; H 8.10; N 2.60. C₃₃H₄₃NO₅. Calculated, %: C 74.27; H 8.12; N 2.62.

3.4. Synthesis of Compounds **45**, **46** and **49**

To a solution containing 1 mmol of compound **36**, **37** or **40** in 5 mL of dimethylformamide, 1.2 mmol (0.09 mL) of propargyl bromide and 2.2 mmol (0.30 g) of K₂CO₃ were added. The reaction mixture was stirred for 18 h and evaporated at room temperature. The residue was diluted with CHCl₃, washed with 5% HCl and water, dried over CaCl₂, and evaporated in a vacuum. The residue was purified by column chromatography, eluent hexane: ethyl acetate, 5:1

Methyl 7-propynyl 1-hydroxy-13-isopropyl-7,10a,2'-trimethyl- 5,6,6b,7,8,9,10,10a, 10b,11,12,13-dodecahydro-12,4b-ethenophenanthro [2,1-g]indole-7,1'-dicarboxylate (**45**). Yield 0.39 g (72%), mp 110–112°C, [α]_{D20} +33.4° (c 0.10, CHCl₃). ¹H NMR spectrum, δ , ppm (J, Hz): 0.81 (3H, s, 18-CH₃); 0.86–0.96 (1H, m, 10-CH₂); 1.02 (3H, d, J = 7.0, 17-CH₃); 1.05 (3H, d, J = 7.0, 16-CH₃); 1.21 (3H, s, 19-CH₃); 1.31–1.69 (10H, m, 6,8,9,10,11-CH₂, 10b-CH); 1.77–1.80 (1H, m, 6b-CH); 1.98–2.18 (1H, m, 15-CH); 2.41–2.48 (1H, m, 5-CH₂); 2.50 (1H, br s., 8'-CH); 2.71 (3H, s, 3'-CH₃); 2.99–3.00 (1H, m, 5-CH₂); 3.91 (3H, s, 5'-CH₃), 4.28 (1H, s, 12-CH); 4.69–4.82 (2H, m, 6'-CH₂); 5.71 (1H, s, 14-CH); 7.28 (1H, s, 2-CH); 6.00 (1H, br. s, OH); 12.01 (1H, br. s, NH). ¹³C NMR spectrum, δ , ppm: 14.9 (C-3'); 16.8 (C-19); 17.1 (C-9), 18.2 (C-18); 20.2 (C-17); 20.5 (C-16); 22.0 (C-6); 28.3 (C-11); 32.2 (C-15); 33.2 (C-5); 36.3 (C-12); 36.9 (C-8); 38.3 (C-4b); 38.8 (C-10); 46.6 (C-7); 47.4 (C-10a); 49.8 (C-6b); 51.4 (C-6'); 52.0 (C-5'); 54.8 (C-10b); 74.4 (C-8'); 78.1 (C-7'); 103.3 (C-2); 108.0 (C-1'); 124.5 (C-3); 127.5 (C-13); 130.9 (C-1a); 133.6 (C-4a); 143.5 (C-4); 146.5 (C-1); 153.2 (C-14); 162.9 (C-2'); 165.6 (C-4'); 178.2 (C-20). Mass spectrum, m/z (I_{rel}, %): 543 [M]+ (100). Found, %: C 75.15; H 7.61; N 2.60. C₃₄H₄₁NO₅. Calculated, %: C 75.11; H 7.60; N 2.58.

Ethyl 7-propynyl 1-hydroxy-13-isopropyl-7,10a,2'-trimethyl- 5,6,6b,7,8,9,10,10a,10b, 11,12,13-dodecahydro-12,4b-ethenophenanthro [2,1-g]indole-7,1'-dicarboxylate (**46**). Yield 0.42 g (75%), mp 98–100°C, [α]_{D20} +2.9° (c 0.15, CHCl₃). ¹H NMR spectrum, δ , ppm (J, Hz): 0.72 (3H, s, 18-CH₃); 0.80–0.96 (1H, m, 10-CH₂); 1.02 (3H, d, J = 7.0, 17-CH₃); 1.05 (3H, d, J = 7.0, 16-CH₃); 1.21 (3H, s, 19-CH₃); 1.31–1.69 (10H, m, 6,8,9,10,11-CH₂,10b-CH); 1.77–1.80 (1H, m, 6b-CH); 1.98–2.18 (1H, m, 15-CH); 2.41–2.48 (1H, m, 9'-CH); 2.65–2.70 (1H,

m, 5-CH₂); 2.73 (3H, s, 3'-CH₃); 2.95–3.05 (1H, m, 5-CH₂); 3.73 (3H, s, 6'-CH₃), 3.95 (1H, s, 12-CH); 4.35–4.42 (2H, m, 5'-CH₂); 4.75 (2H, br. s., 6'-CH₂); 5.70 (1H, s, 14-CH); 7.49 (1H, s, 2-CH); 9.19 (1H, br. s, OH); 12.01 (1H, br. s, NH). ¹³C NMR spectrum, δ , ppm: 14.1 (C-3'); 14.2 (C-19); 14.5 (C-9), 15.9 (C-18); 16.5 (C-17); 16.9 (C-16); 20.2 (C-6); 21.4 (C-11); 22.7 (C-15); 28.3 (C-5); 29.7 (C-12); 32.2 (C-8); 33.2 (C-4b); 36.2 (C-10); 36.9 (C-7); 38.8 (C-10a); 49.9 (C-6b); 51.9 (C-7'); 54.9 (C-6'); 57.1 (C-10b); 60.0 (C-5'), 74.9 (C-9'); 79.3 (C-8'); 101.8 (C-2); 108.6 (C-1'); 124.5 (C-3); 127.6 (C-13); 132.8 (C-1a); 133.8 (C-4a); 144.0 (C-4); 148.6 (C-1); 153.2 (C-14); 162.8 (C-2'); 164.8 (C-4'); 179.5 (C-20). Mass spectrum, m/z (*I*_{rel}, %): 558 [M]⁺ (100). Found, %: C 75.30; H 7.75; N 2.55. C₃₅H₄₃NO₅. Calculated, %: C 75.37; H 7.77; N 2.51.

Propynyl 13-isopropyl-7,10a-dimethyl-1,4-dioxo-4,5,6,6a,7,8,9,10,10a,10b,11,12-dodecahydro-1H-4b,12-ethenochrysene-7-carboxylate (**48**). Yield 0.33 g (75%), mp 85–89 °C, [α]_{D20} +26.9° (c 0.75, CHCl₃). ¹H NMR spectrum, δ , ppm (J, Hz): 0.69 (3H, s, 18-CH₃); 0.86–0.96 (1H, m, 10-CH₂); 1.02 (3H, d, J = 7.0, 17-CH₃); 1.05 (3H, d, J = 7.0, 16-CH₃); 1.21 (3H, s, 19-CH₃); 1.31–1.69 (10H, m, 6,8,9,10,11-CH₂, 10b-CH); 1.77–1.80 (1H, m, 6b-CH); 1.98–2.18 (1H, m, 15-CH); 2.41–2.48 (1H, m, 5-CH₂); 2.50 (1H, br. s, 3'-CH); 2.85–2.89 (1H, m, 5-CH₂); 4.13 (1H, s, 12-CH); 4.67 (2H, br. s, 1'-CH₂); 5.63 (1H, s, 14-CH); 6.45–6.56 (2H, m, 2-CH, 3-CH). ¹³C NMR spectrum, δ , ppm: 16.4 (C-19); 16.8 (C-9), 17.1 (C-18); 20.2 (C-17); 20.6 (C-16); 21.7 (C-6); 27.1 (C-11); 31.5 (C-15); 31.9 (C-5); 36.2 (C-12); 36.4 (C-8); 38.6 (C-4b); 39.3 (C-10); 47.1 (C-7); 49.1 (C-10a); 49.4 (C-6b); 52.1 (C-1'); 54.8 (C-10b); 74.6 (C-3'); 77.9 (C-2'); 127.3 (C-13); 133.6 (C-2); 137.5 (C-3); 150.6 (C-4a); 151.1 (C-14); 152.8 (C-1a); 177.7 (C-20); 184.0 (C-1); 185.3 (C-2). Mass spectrum, m/z (*I*_{rel}, %): 446 [M]⁺ (100). Found, %: C 78.05; H 7.65. C₂₉H₃₄O₄. Calculated, %: C 78.00; H 7.67.

3.5. Synthesis of Compounds **47** and **50**

A mixture of 1 mmol of the compounds **42** or **49**, 20 mmol (1.3 mL) of acrylonitrile and 0.5 mL of 30% KOH per one hydroxyl groups, 0.5 mmol (0.11 g) of BTEAC, in 20 mL of dioxane was stirred for 2 h at room temperature. The mixture was poured into a mixture of ice with HCl, the precipitate was filtered off, washed with water until neutral pH, air dried, and extracted with methylene chloride (3 × 80 mL) with heating, the solution was filtered. The filtrate was evaporated under reduced pressure, and the residue was purified on a silica gel column, eluent hexane–ethyl acetate, 10:1.

Methyl 1-(8'-cyanoethoxy)-13-isopropyl-1'-(ethoxycarbonyl)-7,10a,2'-trimethyl -5,6,6b,7,8,9,10,10a,10b,11,12,13-dodecahydro-12,4b-ethenophenanthro [2,1-g]indole-7-carboxylate (**47**). Yield 0.39 g (68%), mp 127–129 °C, [α]_{D20} +77.9° (c 0.10, CHCl₃). ¹H NMR spectrum, δ , ppm (J, Hz): 0.79 (3H, s, 18-CH₃); 0.86–0.99 (1H, m, 10-CH₂); 1.04 (3H, d, J = 7.0, 17-CH₃); 1.07 (3H, d, J = 7.0, 16-CH₃); 1.24 (3H, s, 19-CH₃); 1.27–1.69 (10H, m, 6,8,9,10,11-CH₂, 10b-CH); 1.77–1.80 (1H, m, 6b-CH); 1.98–2.18 (1H, m, 15-CH); 2.45–2.58 (1H, m, 5-CH₂); 2.76 (3H, s, 3'-CH₃); 2.89–2.91 (2H, m, 7'-CH₂); 2.95–3.15 (1H, m, 5-CH₂); 3.75 (3H, s, 21-CH₃), 3.93 (3H, s, 5'-CH₃), 4.28–4.30 (2H, m, 6'-CH₂); 4.37 (1H, s, 12-CH); 5.72 (1H, s, 14-CH); 7.28 (1H, s, 2-CH); 12.10 (1H, br. s, NH). ¹³C NMR spectrum, δ , ppm: 14.9 (C-3'); 15.5 (C-21), 16.9 (C-19); 16.8 (C-9), 17.2 (C-18); 20.2 (C-17); 20.5 (C-16); 22.1 (C-6); 28.3 (C-11); 32.2 (C-15); 33.2 (C-5); 36.3 (C-12); 36.9 (C-8); 38.4 (C-4b); 38.9 (C-10); 46.7 (C-7); 47.4 (C-10a); 49.9 (C-6b); 51.3 (C-7'); 52.0 (C-5'); 54.9 (C-10b); 63.7 (C-6'), 100.9 (C-2); 108.3 (C-1'); 117.4 (C-8'); 124.6 (C-3); 127.6 (C-13); 133.4 (C-1a); 134.1 (C-4a); 144.0 (C-4); 148.4 (C-1); 153.2 (C-14); 163.0 (C-2'); 165.1 (C-4'); 179.6 (C-20). Mass spectrum, m/z (*I*_{rel}, %): 572 [M]⁺ (100). Found, %: C 73.45; H 7.75; N 4.91. C₃₅H₄₄N₂O₅. Calculated, %: C 73.40; H 7.74; N 4.89.

1,4-Bis(2'-cyanoethoxy)-13-isopropyl-7,10a-dimethyl-6,6a,7,8,9,10,10a,10b,11,12-dodecahydro-5H-4b,12-ethenochrysene-7-carboxylic acid (**50**). Yield 0.41 g (80%), mp 157–159 °C, [α]_{D20} +63.6° (c 0.1, CHCl₃). ¹H NMR spectrum, δ , ppm (J, Hz): 0.79 (3H, s, 18-CH₃); 0.86–0.99 (1H, m, 10-CH₂); 1.08 (3H, d, J = 7.0, 17-CH₃); 1.10 (3H, d, J = 7.0, 16-CH₃); 1.29 (3H, s, 19-CH₃); 1.22–1.69 (10H, m, 6,8,9,10,11-CH₂, 10b-CH); 1.77–1.80 (1H, m, 6b-CH); 1.98–2.18 (1H, m, 15-CH); 2.45–2.58 (1H, m, 5-CH₂); 2.80–2.82 (4H, m, 2'-CH₂, 2''-CH₂); 2.95–3.00 (1H, m, 5-CH₂); 4.05–4.13 (4H, m, 1'-CH₂, 1''-CH₂); 4.24 (1H, s, 12-CH); 5.71 (1H, s, 14-CH); 6.38–6.47 (2H, m, 2-CH, 3-CH); 9.12 (1H, br. s, OH). ¹³C NMR spectrum, δ , ppm: 16.4 (C-19); 16.8

(C-9), 17.2 (C-18); 19.9 (C-2', C-2''); 20.2 (C-17); 20.5 (C-16); 22.1 (C-6); 28.3 (C-11); 32.2 (C-15); 33.2 (C-5); 36.3 (C-12); 36.9 (C-8); 38.4 (C-4b); 38.9 (C-10); 46.6 (C-7); 47.4 (C-10a); 49.9 (C-6b); 54.8 (C-10b); 64.4 (C-1', C-1''); 111.2 (C-1); 114.4 (C-2); 117.6 (C-3', C-3''), 128.6 (C-14); 135.2 (C-4a); 138.4 (C-1a); 145.1 (C-4); 146.0 (C-1); 151.7 (C-13); 185.6 (C-20). Mass spectrum, m/z (I_{rel} , %): 517 [M]+H (100). Found, %: C 74.35; H 7.81; N 5.40. $C_{32}H_{40}N_2O_4$. Calculated, %: C 74.39; H 7.80; N 5.42.

Data of the study α -Gly inhibition in vitro, kinetic, docking studies and ADMET profiling of compound **45**. as well as studies of anti-antioxidant, antimicrobial and cytotoxic activities, can be found in the Supplementary Material (Section S1).

4. Conclusions

The screening of a series of 50 semisynthetic derivatives of levopimaric acid revealed that, in contrast to the majority of previously reported diterpene α -GLy inhibitors, a lead diterpene indole with an alkyne substituent **45** was identified as a competitive inhibitor. As a consequence, one might hope for better translatability to animal and clinical settings, since the active site of yeast α -GLy and intestinal mammalian maltase–glucoamylase are conserved, while allosteric sites are likely to be different. In addition, compound **45** is anticipated to have low intestinal absorption that benefits high concentration of the drug in the target area and helps to avoid systemic exposure. Additional experiments are warranted to confirm antihyperglycemic properties of compound **45** in vivo. In the event of the efficacy and safety being confirmed, novel glucosidase inhibitors open a promising venue to antidiabetic agents able not only to ameliorate postprandial hyperglycemia, but also reduce secretory load on pancreatic beta-cells.

Supplementary Materials: The following supporting information can be downloaded at: <https://www.mdpi.com/article/10.3390/ijms232113535/s1>. Ref [63–71] are cited in Supplementary Materials.

Author Contributions: E.T.—draft preparation; E.T. and I.S. prepared compounds for screening; O.K. brought the idea, managed the research and prepared the manuscript; H.T.T.N., A.S., E.S., D.B. and A.S. (Alina Shevchenko) conducted biological experiments; D.B. and A.S. (Alexander Spasov) prepared the manuscript. All authors have read and agreed to the published version of the manuscript.

Funding: This work was supported by the Federal program (Russian Federation) N^o. 1021062311392-9-1.4.1. Ha Thi Thu Nguyen thanks the Vietnam Academy of Science and Technology (VAST) for support in the screening of compounds against α -glucosidase (Project N^o. QTRU01.05/20-21).

Institutional Review Board Statement: Not applicable.

Informed Consent Statement: Not applicable.

Data Availability Statement: Not applicable.

Conflicts of Interest: The authors declare no conflict of interest.

References

1. Tang, O.; Matsushita, K.; Coresh, J.; Sharrett, A.R.; McEvoy, J.W.; Windham, B.G.; Ballantyne, C.M.; Selvin, E. Mortality implications of prediabetes and diabetes in older adults. *Diabetes Care* **2020**, *43*, 382–388. [[CrossRef](#)]
2. Kitabchi, A.E.; Umpierrez, G.E.; Miles, J.M.; Fisher, J.N. Hyperglycemic crises in adult patients with diabetes. *Diabetes Care* **2009**, *32*, 1335–1343. [[CrossRef](#)]
3. Ceriello, A.; Nicolucci, A. Intensive glucose control and type 2 diabetes—15 years on. *N. Engl. J. Med.* **2019**, *381*, 1292–1293. [[CrossRef](#)]
4. Zheng, Y.; Ley, S.H.; Hu, F.B. Global aetiology and epidemiology of type 2 diabetes mellitus and its complications. *Nat. Rev. Endocrinol.* **2018**, *14*, 88–98. [[CrossRef](#)]
5. Lean, M.; McCombie, L.; McSorely, J. Trends in type 2 diabetes. *BMJ* **2019**, *366*, 15407. [[CrossRef](#)]
6. Williams, J.; Loeffler, M. Global trends in type 2 diabetes, 2007–2017. *JAMA* **2019**, *322*, 1542. [[CrossRef](#)]
7. Bischoff, H. Pharmacology of alpha-glucosidase inhibition. *Eur. J. Clin. Investig.* **1994**, *24*, 3–10.
8. Toeller, M. α -Glucosidase inhibitors in diabetes: Efficacy in NIDDM subjects. *Eur. J. Clin. Investig.* **1994**, *24*, 31–35. [[CrossRef](#)]

9. Soccio, R.E.; Chen, E.R.; Lazar, M.A. Thiazolidinediones and the promise of insulin sensitization in type 2 diabetes. *Cell Metab.* **2014**, *20*, 573–591. [[CrossRef](#)]
10. Ullah, A.; Khan, A.; Khan, I. Diabetes mellitus and oxidative stress—A concise review. *Pharm. J.* **2016**, *24*, 547–553. [[CrossRef](#)]
11. Lorenzati, B.; Zucco, C.; Miglietta, S.; Lamberti, F.; Bruno, G. Oral hypoglycemic drugs: Pathophysiological basis of their mechanism of action. *Pharmaceuticals* **2010**, *3*, 3005–3020. [[CrossRef](#)] [[PubMed](#)]
12. Marín-Peñalver, J.J.; Martín-Timón, I.; Sevillano-Collantes, C.; del Cañizo-Gómez, F.J. Type 2 diabetes and cardiovascular disease: Have all risk factors the same strength. *World J. Diabetes* **2016**, *7*, 354–395. [[CrossRef](#)] [[PubMed](#)]
13. Feliciano, A.S.; Gordaliza, M.; Salinero, M.A.; del Corral, J.M.M. Abietane Acids: Sources, Biological Activities, and Therapeutic Uses. *Planta Med.* **1993**, *59*, 485–490. [[CrossRef](#)] [[PubMed](#)]
14. Tretyakova, E.V.; Smirnova, I.E.; Kazakova, O.B.; Tolstikov, G.A.; Yavorskaya, N.P.; Golubeva, I.S.; Pugacheva, R.B.; Apryshko, G.N.; Poroikov, V.V. Synthesis and anticancer activity of quinopimaric and maleopimaric acids' derivatives. *Bioorg. Med. Chem.* **2014**, *22*, 6481–6489. [[CrossRef](#)] [[PubMed](#)]
15. Tretyakova, E.V.; Smirnova, I.E.; Salimova, E.V.; Odinokov, V.N. Synthesis and antiviral activity of maleopimaric and quinopimaric acids' derivatives. *Bioorg. Med. Chem.* **2015**, *23*, 6543–6550. [[CrossRef](#)]
16. Smirnova, I.E.; Tretyakova, E.V.; Baev, D.S.; Kazakova, O.B. Synthetic modifications of abietane diterpene acids to potent antimicrobial agents. *Nat. Prod. Res.* **2021**, 1–9. [[CrossRef](#)]
17. Kim, E.; Kang, Y.-G.; Kim, Y.-J.; Lee, T.R.; Yoo, B.C.; Jo, M.; Kim, J.H.; Kim, J.H.; Kim, D.; Cho, J.Y. Dehydroabietic acid suppresses inflammatory response via suppression of Src-, Syk-, and TAK1-mediated pathways. *Int. J. Mol. Sci.* **2019**, *20*, 1593. [[CrossRef](#)]
18. Tretyakova, E.V.; Salimova, E.V.; Parfenova, L.V. Synthesis, modification, and biological activity of propargylated methyl dihydroquinopimarates. *Nat. Prod. Res.* **2022**, *36*, 79–86. [[CrossRef](#)]
19. Goncalves, M.D.; Bortoleti, B.T.S.; Tomiotto-Pellissier, F.; Miranda-Sapla, M.M.; Assolini, J.P.; Carlotto, A.C.M.; Carvalho, P.G.C.; Tudisco, E.T.; Urbano, A.; Ambrosio, S.R.; et al. Dehydroabietic acid isolated from *Pinus elliottii* exerts in vitro antileishmanial action by pro-oxidant effect, inducing ROS production in promastigote and downregulating Nrf2/ferritin expression in amastigote forms of *Leishmania amazonensis*. *Fitoterapia* **2018**, *128*, 224–232. [[CrossRef](#)]
20. González, M.A. Aromatic abietane diterpenoids: Their biological activity and synthesis. *Nat. Prod. Rep.* **2015**, *32*, 684–704. [[CrossRef](#)]
21. Etsassala, N.G.E.R.; Cupido, C.N.; Iwuoha, I.E.; Hussein, A.A. Abietane Diterpenes as Potential Candidates for the Management of Type 2 Diabetes. *Curr. Pharm. Des.* **2020**, *26*, 2885–2891. [[CrossRef](#)] [[PubMed](#)]
22. Nachar, A.; Saleem, A.; Arnason, J.T.; Haddad, P.S. Regulation of liver cell glucose homeostasis by dehydroabietic acid, abietic acid and squalene isolated from balsam fir (*Abies balsamea* (L.) Mill.) a plant of the Eastern James Bay Cree traditional pharmacopeia. *Phytochemistry* **2015**, *117*, 373–379. [[CrossRef](#)] [[PubMed](#)]
23. Song, H.M.; Li, X.; Liu, Y.Y.; Lu, W.-P.; Cui, Z.-H.; Zhou, L.; Yao, D.; Zhang, H.-M. Carnosic acid protects mice from high-fat diet-induced NAFLD by regulating MARCKS. *Int. J. Mol. Med.* **2018**, *42*, 193–207. [[CrossRef](#)] [[PubMed](#)]
24. Lipina, C.; Hundal, H.S. Carnosic acid stimulates glucose uptake in skeletal muscle cells via a PME-1/PP2A/PKB signalling axis. *Cell. Signal.* **2014**, *26*, 2343–2349. [[CrossRef](#)] [[PubMed](#)]
25. Christensen, K.B.; Jørgensen, M.; Kotowska, D.; Petersen, R.K.; Kristiansen, K.; Christensen, L.P. Activation of the nuclear receptor PPAR γ by metabolites isolated from sage (*Salvia officinalis* L.). *J. Ethnopharmacol.* **2010**, *132*, 127–133. [[CrossRef](#)] [[PubMed](#)]
26. Xie, Z.; Gao, G.; Wang, H.; Lia, E.; Yuan, Y.; Xu, J.; Zhang, Z.; Wang, P.; Fu, Y.; Zeng, H.; et al. Dehydroabietic acid alleviates high fat diet-induced insulin resistance and hepatic steatosis through dual activation of PPAR- γ and PPAR- α . *Biomed. Pharmacother.* **2020**, *127*, 110155. [[CrossRef](#)]
27. Vlavcheski, F.; Baron, D.; Vlachogiannis, I.A.; MacPherson, R.E.K.; Tsiani, E. Carnosol increases skeletal muscle cell glucose uptake via AMPK-Dependent GLUT4 glucose transporter translocation. *Int. J. Mol. Sci.* **2018**, *19*, 1321. [[CrossRef](#)]
28. Samarghandian, S.; Borji, A.; Farkhondeh, T. Evaluation of antidiabetic activity of carnosol (phenolic diterpene in rosemary) in Streptozotocin-induced diabetic rats. *Cardiovasc. Hematol. Disord. Drug Targets* **2017**, *17*, 11–17. [[CrossRef](#)]
29. Cui, L.; Kim, M.O.; Seo, J.H.; Kim, I.S.; Kim, N.Y.; Lee, S.H.; Park, J.; Kim, J.; Lee, H.S. Abietane diterpenoids of *Rosmarinus officinalis* and their diacylglycerol acyltransferase-inhibitory activity. *Food Chem.* **2012**, *132*, 1775–1780. [[CrossRef](#)]
30. Yun, Y.S.; Noda, S.; Shigemori, G.; Kuriyama, R.; Takahashi, S.; Umemura, M.; Takahashi, Y.; Inoue, H. Phenolic diterpenes from rosemary suppress cAMP responsiveness of gluconeogenic gene promoters. *Phytother. Res.* **2013**, *27*, 906–910. [[CrossRef](#)]
31. Kubínová, R.; Pořízková, R.; Navrátilová, A.; Farsa, O.; Hanáková, Z.; Bačinská, A.; Cížek, A.; Valentová, M. Antimicrobial and enzyme inhibitory activities of the constituents of *Plectranthus madagascariensis* (Pers.) Benth. *J. Enzym. Inhib. Med. Chem.* **2014**, *29*, 749–752. [[CrossRef](#)] [[PubMed](#)]
32. Kim, D.H.; Paudel, P.; Yu, T.; Ngo, T.M.; Kim, J.A.; Jung, H.A.; Yokozawa, T.; Choi, J.S. Characterization of the inhibitory activity of natural tanshinones from *Salvia miltiorrhiza* roots on protein tyrosine phosphatase 1B. *Chem. Biol. Interact.* **2017**, *278*, 65–73. [[CrossRef](#)] [[PubMed](#)]
33. Jung, S.H.; Seol, H.J.; Jeon, S.J.; Son, K.H.; Lee, J.R. Insulin-sensitizing activities of tanshinones, diterpene compounds of the root of *Salvia miltiorrhiza* Bunge. *Phytomedicine* **2009**, *16*, 327–335. [[CrossRef](#)] [[PubMed](#)]
34. Kang, M.S.; Hirai, S.; Goto, T.; Kuroyanagi, K.; Kim, Y.-I.; Ohyama, K.; Uemura, T.; Lee, J.-Y.; Sakamoto, T.; Ezaki, Y.; et al. Dehydroabietic acid, a diterpene, improves diabetes and hyperlipidemia in obese diabetic KK-Ay mice. *Biofactors* **2009**, *35*, 442–448. [[CrossRef](#)] [[PubMed](#)]

35. Ou, J.; Huang, J.; Zhao, D.; Du, B.; Wang, M. Protective effect of rosmarinic acid and carnosic acid against streptozotocin-induced oxidation, glycation, inflammation and microbiota imbalance in diabetic rats. *Food Funct.* **2018**, *9*, 851–860. [[CrossRef](#)] [[PubMed](#)]
36. Wei, Y.; Gao, J.; Qin, L.; Xu, Y.; Wang, D.; Shi, H.; Xu, T.; Liu, T. Tanshinone I alleviates insulin resistance in type 2 diabetes mellitus rats through IRS-1 pathway. *Biomed. Pharmacother.* **2017**, *93*, 352–358. [[CrossRef](#)]
37. Allen, G.R., Jr. *Organic Reactions*; Wiley: New York, NY, USA, 1973; Volume 20, p. 338.
38. Tretyakova, E.V.; Yarmukhametova, L.R.; Salimova, E.V.; Kukovinets, O.S.; Parfenova, L.V. The Nenitzescu reaction in the synthesis of new abietane diterpene indoles. *Chem. Heterocycl. Compd.* **2020**, *56*, 1366–1369. [[CrossRef](#)]
39. Tran, C.-L.; Dao, T.-B.-N.; Tran, T.-N.; Mai, D.-T.; Tran, T.-M.-D.; Tran, N.-M.-A.; Dang, V.-S.; Vo, T.-X.; Duong, T.-H.; Sichaem, J. Alpha-Glucosidase Inhibitory Diterpenes from *Euphorbia antiquorum* Growing in Vietnam. *Molecules* **2021**, *26*, 2257. [[CrossRef](#)]
40. Ghosh, S.; Rangan, L. Molecular Docking and Inhibition Kinetics of α -glucosidase Activity by Labdane Diterpenes Isolated from Tora Seeds (*Alpinia nigra* B.L. Burt.). *Appl. Biochem. Biotechnol.* **2015**, *175*, 1477–1489. [[CrossRef](#)]
41. Yang, X.-T.; Geng, C.-A.; Li, T.-Z.; Deng, Z.-T.; Chen, J.-J. Synthesis and biological evaluation of chepraecoxin A derivatives as α -glucosidase inhibitors. *Bioorg. Med. Chem. Lett.* **2020**, *30*, 127020. [[CrossRef](#)]
42. Loo, K.Y.; Leong, K.H.; Sivasothy, Y.; Ibrahim, H.; Awang, K. Molecular Insight and Mode of Inhibition of α -Glucosidase and α -Amylase by Pahangensin A from *Alpinia pahangensis* Ridl. *Chem. Biodivers.* **2019**, *16*, e1900032. [[CrossRef](#)] [[PubMed](#)]
43. Ma, Y.-Y.; Zhao, D.-G.; Zhang, R.; He, X.; Li, B.Q.; Zhang, X.-Z.; Wang, Z.; Zhang, K. Identification of bioactive compounds that contribute to the α -glucosidase inhibitory activity of rosemary. *Food Funct.* **2020**, *11*, 1692–1701. [[CrossRef](#)] [[PubMed](#)]
44. Bissantz, C.; Kuhn, B.; Stahl, M. A medicinal chemist's guide to molecular interactions. *J. Med. Chem.* **2010**, *53*, 5061–5084. [[CrossRef](#)] [[PubMed](#)]
45. Stein, R.L. *Kinetics of Enzyme Action: Essential Principles for Drug Hunters*; John Wiley & Sons: Hoboken, NJ, USA, 2011.
46. Dong, J.; Wang, N.-N.; Yao, Z.-J.; Zhang, L.; Cheng, Y.; Ouyang, D.; Lu, A.-P.; Cao, D.-S. ADMETlab: A platform for systematic ADMET evaluation based on a comprehensively collected ADMET database. *J. Cheminform.* **2018**, *10*, 29. [[CrossRef](#)] [[PubMed](#)]
47. Xiong, G.; Wu, Z.; Yi, J.; Fu, L.; Yang, Z.; Hsieh, C.; Yin, M.; Zeng, X.; Wu, C.; Lu, A.; et al. ADMETlab 2.0: An integrated online platform for accurate and comprehensive predictions of ADMET properties. *Nucleic Acids Res.* **2021**, *49*, W5–W14. [[CrossRef](#)] [[PubMed](#)]
48. Daina, A.; Michielin, O.; Zoete, V. SwissADME: A free web tool to evaluate pharmacokinetics, drug-likeness and medicinal chemistry friendliness of small molecules. *Sci. Rep.* **2017**, *7*, 42717. [[CrossRef](#)]
49. Banerjee, P.; Eckert, A.O.; Schrey, A.K.; Preissner, R. ProTox-II: A webserver for the prediction of toxicity of chemicals. *Nucleic Acids Res.* **2018**, *46*, W257–W263. [[CrossRef](#)]
50. Herz, W.; Blackstone, R.C.; Nair, M.G. Resin acids. XI Configuration and transformations of the levopimaric acid-p-benzoquinone adduct. *J. Org. Chem.* **1967**, *32*, 2992–2998. [[CrossRef](#)]
51. Smirnova, I.E.; Tretyakova, E.V.; Flekhter, O.B.; Spirikhin, L.V.; Galin, F.Z.; Tolstikov, G.A.; Starikova, Z.A.; Korlyukov, A.A. Synthesis, structure, and acylation of dihydroquinopimaric acid hydroxyl derivatives. *Russ. J. Org. Chem.* **2008**, *44*, 1598–1605. [[CrossRef](#)]
52. Smirnova, I.E.; Tretyakova, E.V.; Kazakova, O.B.; Starikova, Z.A.; Fedyanin, I.V. Molecular and crystal structure of a new compound methyl-18R-13-isopropyl-10a,7-dimethyl-4-oxo-1-oxahexacyclo[12.4.0.0^{5a,4a}.0^{13,12}.0^{010a,6a}]heneicosane-7-Carboxylate. *J. Struct. Chem.* **2009**, *50*, 378–380. [[CrossRef](#)]
53. Smirnova, I.E.; Tretyakova, E.V.; Kazakova, O.B.; Suponitsky, K.Y. Molecular structure of methyl 20-isopropyl-15(e)-hydroxyimino-5,9-dimethyl-18-oxahexacyclo[12.4.0.2¹³.1^{18,20}.0^{5,10}.0^{4,13}]heneicosane-9-carboxylate. *J. Struct. Chem.* **2010**, *51*, 1208–1210. [[CrossRef](#)]
54. Tretyakova, E.V.; Salimova, E.V.; Odinkov, V.N.; Dzhemilev, U.M. Synthesis of a Novel 1,2,4-Oxadiazole Diterpene from the Oxime of the Methyl Ester of 1 β ,13-Epoxydihydroquinopimaric Acid. *Nat. Prod. Commun.* **2016**, *11*, 23–24. [[CrossRef](#)] [[PubMed](#)]
55. Kazakova, O.B.; Tretyakova, E.V.; Smirnova, I.E.; Spirikhin, L.V.; Tolstikov, G.A.; Chudov, I.V.; Bazekin, G.V.; Ismagilova, A.F. The synthesis and anti-inflammatory activity of quinopimaric acid derivatives. *Russ. J. Bioorg. Chem.* **2010**, *36*, 257–262. [[CrossRef](#)] [[PubMed](#)]
56. Tretyakova, E.V.; Salimova, E.V.; Parfenova, L.V.; Odinkov, V.N. Synthesis and Modifications of Alkyne Derivatives of Dihydroquinopimaric, Maleopimaric, and Fumaropimaric Acids. *Russ. J. Org. Chem.* **2016**, *52*, 1496–1502. [[CrossRef](#)]
57. Flekhter, O.B.; Smirnova, I.E.; Tretyakova, E.V.; Tolstikov, G.A.; Savinova, O.V.; Boreko, E.I. Synthesis of Dihydroquinopimaric Acid Conjugates with Amino Acids. *Russ. J. Bioorg. Chem.* **2009**, *35*, 385–390. [[CrossRef](#)]
58. Tretyakova, E.V.; Salimova, E.V.; Parfenova, L.V.; Yunusbaeva, M.M.; Dzhemileva, L.U.; D'yakonov, V.A.; Dzhemilev, U.M. Synthesis of New Dihydroquinopimaric Acid Analogs with Nitrile Groups as Apoptosis-Inducing Anticancer Agents. *Anti-Cancer Agents Med. Chem.* **2019**, *19*, 1172–1183. [[CrossRef](#)]
59. Smirnova, I.E.; Kazakova, O.B.; Tretyakova, E.V.; Spirikhin, L.V.; Glukhov, I.V.; Nelyubina, Y.V. Regioselective Bromination of Quinopimaric Acid Derivatives. *Russ. J. Org. Chem.* **2010**, *46*, 1135–1139. [[CrossRef](#)]
60. Kazakova, O.B.; Tretyakova, E.V.; Smirnova, I.E.; Nazyrov, T.I.; Kukovinets, O.S.; Tolstikov, G.A.; Suponitskii, K.Y. An efficient oxyfunctionalization of quinopimaric acid derivatives with ozone. *Nat. Prod. Commun.* **2013**, *28*, 293–296.
61. Smirnova, I.E.; Kazakova, O.B.; Tretyakova, E.V.; Tolstikov, G.A.; Spirikhin, L.V. Synthesis of Heterocyclic Derivatives of Dihydroquinopimaric Acid. *Russ. J. Org. Chem.* **2011**, *47*, 1576–1580. [[CrossRef](#)]

62. Shul'ts, E.E.; Oleinikov, D.S.; Nechepurenko, I.V.; Shakirov, M.M.; Tolstikov, G.A. Synthetic transformations of higher terpenoids: XVIII. Synthesis of optically active 9,10-anthraquinone derivatives. *Russ. J. Org. Chem.* **2009**, *45*, 102–114. [[CrossRef](#)]
63. Ha, N.T.T.; van Cuong, P.; Tra, N.T.; Anh, I.T.; Cham, B.T.; Son, N.T. Chemical constituents from methanolic extract of *Garcinia mackeaniana* leaves and their antioxidant activity. *Vietnam. J. Sci. Technol.* **2020**, *58*, 411–418.
64. Ha, N.T.T.; van Cuong, P.; Anh, I.T.; Tra, N.T.; Cham, B.T.; Son, N.T. Antimicrobial xanthenes from *Garcinia mackeaniana* leaves. *Vietnam J. Chem.* **2020**, *58*, 343–348. [[CrossRef](#)]
65. Mosmann, T. Rapid colorimetric assay for cellular growth and survival: Application to proliferation and cytotoxicity assays. *J. Immunol. Methods* **1983**, *65*, 55–63. [[CrossRef](#)]
66. Kim, Y.M.; Wang, M.H.; Rhee, H.I. A novel α -glucosidase inhibitor from pine bark. *Carbohydr. Res.* **2004**, *339*, 715–717. [[CrossRef](#)] [[PubMed](#)]
67. Li, T.; Zhang, X.D.; Song, Y.W.; Liu, J.W. A microplate-based screening method for α -glucosidase inhibitors. *Nat. Prod. Res. Dev.* **2005**, *10*, 1128–1134.
68. *MarvinSketch*, 18.8.0; ChemAxon Ltd.: Budapest, Hungary, 2018.
69. Spasov, A.A.; Babkov, D.A.; Osipov, D.V.; Klochkov, V.G.; Prilepskaya, D.R.; Demidov, M.R.; Osyanin, V.A.; Klimochkin, Y.N. Synthesis, in vitro and in vivo evaluation of 2-aryl-4H-chromene and 3-aryl-1H-benzo[f]chromene derivatives as novel α -glucosidase inhibitors. *Bioorg. Med. Chem. Lett.* **2019**, *29*, 119–123. [[CrossRef](#)]
70. Trott, O.; Olson, A.J. AutoDock Vina: Improving the speed and accuracy of docking with a new scoring function, efficient optimization, and multithreading. *J. Comput. Chem.* **2009**, *31*, 455–461. [[CrossRef](#)]
71. *Discovery Studio Visualizer*, 17.2.0.16349; Dassault Systemes Biovia Corp.: San Diego, CA, USA, 2016.